EUROPEAN ORGANIZATION FOR NUCLEAR RESEARCH

Search for Dirac Magnetic Monopoles
in e$^+$e$^-$ Collisions
with the OPAL Detector at LEP2

The OPAL Collaboration

Abstract

This letter describes a direct search for pair produced magnetic monopoles in e$^+$e$^-$ collisions. The analysis is based on 62.7 pb^{-1} of data collected with the OPAL detector at an average centre-of-mass energy of $\sqrt{s}$= 206.3 GeV. The monopole signal was assumed to be characterized by two back-to-back particles with an anomalously high ionization energy loss dE/dx in the tracking chambers. No evidence for production of monopoles was observed. Upper limits were obtained on the magnetic monopole pair-production cross-section (σ) in the mass range 45 GeV/c^2 < m_M < 102 GeV/c^2. The average limit is σ < 0.05 pb and is essentially independent of the magnetic monopole mass. The cross-section limit is derived at the 95% confidence level and is valid for spin-1/2 magnetic monopoles.

arXiv:0707.0404v1 [hep-ex] 3 Jul 2007

The OPAL Collaboration

G. Abbiendi[2], C. Ainsley[5], P.F. Åkesson[7], G. Alexander[21], G. Anagnostou[1], K.J. Anderson[8], S. Asai[22], D. Axen[26], I. Bailey[25], E. Barberio[7,p], T. Barillari[31], R.J. Barlow[15], R.J. Batley[5], P. Bechtle[24], T. Behnke[24], K.W. Bell[19], P.J. Bell[1], G. Bella[21], A. Bellerive[6], G. Benelli[4], S. Bethke[31], O. Biebel[30], O. Boeriu[9], P. Bock[10], M. Boutemeur[30], S. Braibant[2], R.M. Brown[19], H.J. Burckhart[7], S. Campana[4], P. Capiluppi[2], R.K. Carnegie[6], A.A. Carter[12], J.R. Carter[5], C.Y. Chang[16], D.G. Charlton[1], C. Ciocca[2], A. Csilling[28], M. Cuffiani[2], S. Dado[20], G.M. Dallavalle[2], A. De Roeck[7], E.A. De Wolf[7,s], K. Desch[24], B. Dienes[29], J. Dubbert[30], E. Duchovni[23], G. Duckeck[30], I.P. Duerdoth[15], E. Etzion[21], F. Fabbri[2], P. Ferrari[7], F. Fiedler[30], I. Fleck[9], M. Ford[15], A. Frey[7], P. Gagnon[11], J.W. Gary[4], C. Geich-Gimbel[3], G. Giacomelli[2], P. Giacomelli[2], M. Giunta[4], J. Goldberg[20], E. Gross[23], J. Grunhaus[21], M. Gruwé[7], A. Gupta[8], C. Hajdu[28], M. Hamann[24], G.G. Hanson[4], A. Harel[20], M. Hauschild[7], C.M. Hawkes[1], R. Hawkings[7], G. Herten[9], R.D. Heuer[24], J.C. Hill[5], D. Horváth[28,c], P. Igo-Kemenes[10], K. Ishii[22], H. Jeremie[17], P. Jovanovic[1], T.R. Junk[6,i], J. Kanzaki[22,u], D. Karlen[25], K. Kawagoe[22], T. Kawamoto[22], R.K. Keeler[25], R.G. Kellogg[16], B.W. Kennedy[19], S. Kluth[31], T. Kobayashi[22], M. Kobel[3,t], S. Komamiya[22], T. Krämer[24], A. Krasznahorkay Jr.[29,e], P. Krieger[6,l], J. von Krogh[10], T. Kuhl[24], M. Kupper[23], G.D. Lafferty[15], H. Landsman[20], D. Lanske[13], D. Lellouch[23], J. Letts[o], L. Levinson[23], J. Lillich[9], S.L. Lloyd[12], F.K. Loebinger[15], J. Lu[26,b], A. Ludwig[3,t], J. Ludwig[9], W. Mader[3,t], S. Marcellini[2], A.J. Martin[12], T. Mashimo[22], P. Mättig[m], J. McKenna[26], R.A. McPherson[25], F. Meijers[7], W. Menges[24], F.S. Merritt[8], H. Mes[6,a], N. Meyer[24], A. Michelini[2], S. Mihara[22], G. Mikenberg[23], D.J. Miller[14], W. Mohr[9], T. Mori[22], A. Mutter[9], K. Nagai[12], I. Nakamura[22,v], H. Nanjo[22], H.A. Neal[32], S.W. O'Neale[1,*], A. Oh[7], M.J. Oreglia[8], S. Orito[22,*], C. Pahl[31], G. Pásztor[4,g], J.R. Pater[15], J.E. Pilcher[8], J. Pinfold[27], D.E. Plane[7], O. Pooth[13], M. Przybycień[7,n], A. Quadt[31], K. Rabbertz[7,r], C. Rembser[7], P. Renkel[23], J.M. Roney[25], A.M. Rossi[2], Y. Rozen[20], K. Runge[9], K. Sachs[6], T. Saeki[22], E.K.G. Sarkisyan[7,j], A.D. Schaile[30], O. Schaile[30], P. Scharff-Hansen[7], J. Schieck[31], T. Schörner-Sadenius[7,z], M. Schröder[7], M. Schumacher[3], R. Seuster[13,f], T.G. Shears[7,h], B.C. Shen[4], P. Sherwood[14], A. Skuja[16], A.M. Smith[7], R. Sobie[25], S. Söldner-Rembold[15], F. Spano[8,x], A. Stahl[13], D. Strom[18], R. Ströhmer[30], S. Tarem[20], M. Tasevsky[7,d], R. Teuscher[8], M.A. Thomson[5], E. Torrence[18], D. Toya[22], I. Trigger[7,w], Z. Trócsányi[29,e], E. Tsur[21], M.F. Turner-Watson[1], I. Ueda[22], B. Ujvári[29,e], C.F. Vollmer[30], P. Vannerem[9], R. Vértesi[29,e], M. Verzocchi[16], H. Voss[7,q], J. Vossebeld[7,h], C.P. Ward[5], D.R. Ward[5], P.M. Watkins[1], A.T. Watson[1], N.K. Watson[1], P.S. Wells[7], T. Wengler[7], N. Wermes[3], G.W. Wilson[15,k], J.A. Wilson[1], G. Wolf[23], T.R. Wyatt[15], S. Yamashita[22], D. Zer-Zion[4], L. Zivkovic[20]

[1]School of Physics and Astronomy, University of Birmingham, Birmingham B15 2TT, UK
[2]Dipartimento di Fisica dell' Università di Bologna and INFN, I-40126 Bologna, Italy
[3]Physikalisches Institut, Universität Bonn, D-53115 Bonn, Germany
[4]Department of Physics, University of California, Riverside CA 92521, USA
[5]Cavendish Laboratory, Cambridge CB3 0HE, UK
[6]Ottawa-Carleton Institute for Physics, Department of Physics, Carleton University, Ottawa, Ontario K1S 5B6, Canada
[7]CERN, European Organisation for Nuclear Research, CH-1211 Geneva 23, Switzerland

[8]Enrico Fermi Institute and Department of Physics, University of Chicago, Chicago IL 60637, USA

[9]Fakultät für Physik, Albert-Ludwigs-Universität Freiburg, D-79104 Freiburg, Germany

[10]Physikalisches Institut, Universität Heidelberg, D-69120 Heidelberg, Germany

[11]Indiana University, Department of Physics, Bloomington IN 47405, USA

[12]Queen Mary and Westfield College, University of London, London E1 4NS, UK

[13]Technische Hochschule Aachen, III Physikalisches Institut, Sommerfeldstrasse 26-28, D-52056 Aachen, Germany

[14]University College London, London WC1E 6BT, UK

[15]School of Physics and Astronomy, Schuster Laboratory, The University of Manchester M13 9PL, UK

[16]Department of Physics, University of Maryland, College Park, MD 20742, USA

[17]Laboratoire de Physique Nucléaire, Université de Montréal, Montréal, Québec H3C 3J7, Canada

[18]University of Oregon, Department of Physics, Eugene OR 97403, USA

[19]Rutherford Appleton Laboratory, Chilton, Didcot, Oxfordshire OX11 0QX, UK

[20]Department of Physics, Technion-Israel Institute of Technology, Haifa 32000, Israel

[21]Department of Physics and Astronomy, Tel Aviv University, Tel Aviv 69978, Israel

[22]International Centre for Elementary Particle Physics and Department of Physics, University of Tokyo, Tokyo 113-0033, and Kobe University, Kobe 657-8501, Japan

[23]Particle Physics Department, Weizmann Institute of Science, Rehovot 76100, Israel

[24]Universität Hamburg/DESY, Institut für Experimentalphysik, Notkestrasse 85, D-22607 Hamburg, Germany

[25]University of Victoria, Department of Physics, P O Box 3055, Victoria BC V8W 3P6, Canada

[26]University of British Columbia, Department of Physics, Vancouver BC V6T 1Z1, Canada

[27]University of Alberta, Department of Physics, Edmonton AB T6G 2J1, Canada

[28]Research Institute for Particle and Nuclear Physics, H-1525 Budapest, P O Box 49, Hungary

[29]Institute of Nuclear Research, H-4001 Debrecen, P O Box 51, Hungary

[30]Ludwig-Maximilians-Universität München, Sektion Physik, Am Coulombwall 1, D-85748 Garching, Germany

[31]Max-Planck-Institute für Physik, Föhringer Ring 6, D-80805 München, Germany

[32]Yale University, Department of Physics, New Haven, CT 06520, USA

[a] and at TRIUMF, Vancouver, Canada V6T 2A3

[b] now at University of Alberta

[c] and Institute of Nuclear Research, Debrecen, Hungary

[d] now at Institute of Physics, Academy of Sciences of the Czech Republic 18221 Prague, Czech Republic

[e] and Department of Experimental Physics, University of Debrecen, Hungary

[f] and MPI München

[g] and Research Institute for Particle and Nuclear Physics, Budapest, Hungary

[h] now at University of Liverpool, Dept of Physics, Liverpool L69 3BX, U.K.

[i] now at Dept. Physics, University of Illinois at Urbana-Champaign, U.S.A.

[j] and The University of Manchester, M13 9PL, United Kingdom

[k] now at University of Kansas, Dept of Physics and Astronomy, Lawrence, KS 66045, U.S.A.

[l] now at University of Toronto, Dept of Physics, Toronto, Canada

[m] current address Bergische Universität, Wuppertal, Germany

[n] now at University of Mining and Metallurgy, Cracow, Poland

^{o} now at University of California, San Diego, U.S.A.

^{p} now at The University of Melbourne, Victoria, Australia

^{q} now at IPHE Université de Lausanne, CH-1015 Lausanne, Switzerland

^{r} now at IEKP Universität Karlsruhe, Germany

^{s} now at University of Antwerpen, Physics Department,B-2610 Antwerpen, Belgium; supported by Interuniversity Attraction Poles Programme – Belgian Science Policy

^{t} now at Technische Universität, Dresden, Germany

^{u} and High Energy Accelerator Research Organisation (KEK), Tsukuba, Ibaraki, Japan

^{v} now at University of Pennsylvania, Philadelphia, Pennsylvania, USA

^{w} now at TRIUMF, Vancouver, Canada

^{x} now at Columbia University

^{y} now at CERN

^{z} now at DESY

* Deceased

1 Introduction

In 1931 Dirac linked the existence of magnetic monopoles (MMs) with the quantization of electric charge and postulated the relation between the elementary electric charge e of the electron and a basic magnetic charge g [1]:

$$g = \frac{n\hbar c}{2e} = ng_D, \qquad n = 1, 2, ... \tag{1}$$

where n is an unknown integer and $g_D = \hbar c/2e = 68.5e$ is the unit Dirac magnetic charge (in the cgs system). If free quarks exist, Eq. 1 should be modified by replacing e with $e/3$, which effectively increases g by a factor of 3. There was no prediction for the monopole mass. A rough estimate, obtained assuming that the classical monopole radius is equal to the classical electron radius, yields $m_M \approx g^2 m_e/e^2 \approx n^2 \cdot 4700 m_e \approx n^2 \cdot 2.4 \text{ GeV}/c^2$. Since 1931, experimental searches for "classical Dirac" monopoles have been performed at nearly every new high-energy accelerator, employing a variety of direct and indirect methods [2]. By a classical (Dirac) monopole, we mean a particle without electric charge or hadronic interactions and with magnetic charge g satisfying the Dirac quantization condition (Eq. 1).

Within the framework of Grand Unified Theories (GUT) of the strong and electroweak interactions, supermassive magnetic monopoles with masses $m \geq 10^{16} \text{ GeV}/c^2$ could have been produced in the early Universe as intrinsically stable topological defects at a high energy phase transition that leaves an unbroken U(1) group [3]. At the present time, such monopoles could exist in the penetrating cosmic radiation as "fossil" remnants of that transition. The detection of such particles would be one of the most spectacular confirmations of GUT predictions. The most stringent upper limits on an isotropic flux of GUT magnetic monopoles, assuming monopole masses $m_M > 10^{16} \text{ GeV}/c^2$, have been set by the MACRO experiment [4]. In some Grand Unified theories values of the monopole mass as low as $10^4 \text{ GeV}/c^2$ are allowed [5,6]. Although it is not yet possible to set direct limits at this mass scale, it is worthwhile to search in the accessible region at LEP energies.

Searches for classical point-like monopoles have been performed mainly at high-energy accelerators and in cosmic radiation experiments. Monopole searches have predominantly used either ionization or induction detection techniques.

Induction experiments measure the monopole magnetic charge and are independent of monopole mass and velocity. These experiments search for the induction of a persistent current within a superconducting loop [7]. Searches for magnetic monopoles using this method have been performed at the p$\bar{\text{p}}$ Tevatron collider assuming that produced MMs could stop, and be trapped and bound, in the matter surrounding the D0 and CDF collision regions [8]. The same strategy has been used to search for magnetic monopoles produced in e$^+$p collisions at HERA [9].

Ionization experiments rely on the large magnetic charge of monopoles to produce more ionization than an electrical charge travelling with the same velocity. For $g = g_D$ and velocities $\beta = (v/c) \geq 10^{-2}$ a magnetic monopole behaves, in terms of ionization energy loss (dE/dx), like an equivalent electric charge with $(ze)_{eq} = g_D\beta$. The energy losses are thus very large

$$(dE/dx)_g = (g\beta/e)^2(dE/dx)_e \tag{2}$$

and Dirac magnetic monopoles would be easily distinguished from minimum ionizing electrically charged Standard Model (SM) particles [10–12]. Direct searches for magnetic monopoles using tracking devices were performed at p$\bar{\text{p}}$ and e$^+$e$^-$ colliders. Experiments at the Tevatron collider established cross section limits of about 2×10^{-34} cm^2 for MMs with $m_M < 850$ GeV/c^2 [13], while searches at LEP have excluded masses up to 45 GeV/c^2 [14].

Indirect searches for classical monopoles have relied on the effects of virtual monopole/anti-monopole loops added to QED processes in p$\bar{\text{p}}$ and e$^+$e$^-$ collisions [15, 16]. Since the Standard Model Z^{0}boson could couple to monopoles, assuming that the coupling between the Z^0 and a MM pair is larger than for any lepton pair, the measurement of the Z^0 decay width provides an indirect limit on MM production for $m_M < m_Z/2$ [6, 12].

This paper describes a direct search for MM pairs produced in e$^+$e$^- \rightarrow M\bar{M}(\gamma)$ reactions. The data were collected with the OPAL detector at the LEP accelerator at CERN. This search was primarily based on the dE/dx measurements in the tracking chambers. OPAL has a well established analysis to search for stable, long-lived, massive particles using the dE/dx signatures of individual charged particle tracks [17]. This analysis technique could not be used here because MMs are too heavily ionizing, resulting in charge saturation in the central jet chamber. Therefore, a new analysis method was developed based on hit information rather than reconstructed tracks. The analysis was sensitive to MMs with masses from 45 GeV/c^2 up to the kinematic limit (about 103 GeV/c^2).

2　The OPAL Detector

A description of the OPAL detector and its jet chamber can be found in reference [18]. Only a brief overview is given here.

The OPAL detector operated at LEP between 1989 and 2000 and is now dismantled. The central detector comprised a system of tracking chambers, providing track reconstruction over 96% of the full solid angle[1] inside a 0.435 T uniform magnetic field parallel to the beam axis. It consisted of a two-layer silicon microstrip vertex detector, a high-precision vertex drift chamber with axial and stereo wires, a large-volume jet chamber and a set of z-chambers measuring the track coordinates along the beam direction.

---

[1]The OPAL right-handed coordinate system is defined such that the z-axis is in the direction of the electron beam, the x-axis points toward the centre of the LEP ring, and θ and ϕ are the polar and azimuthal angles, defined relative to the $+z$- and $+x$-axes, respectively. The radial coordinate is denoted by r.

The jet chamber (CJ) [19] is the most important detector for this analysis. The chamber, with a diameter of about 2m and a length of about 4m, was divided into 24 azimuthal sectors, each equipped with 159 sense wires. Up to 159 position and dE/dx measurements per track were thus possible.

The CJ also provided the hardware trigger for monopole candidates. This trigger identified events with highly ionizing particles. Of the 159 sense wires of a sector, 36 wires were combined to define three groups with 12 wires each. One group was at an inner region, close to the e^+e^- collision axis. The other two groups were at central and outer regions. For each wire, hits from highly ionizing tracks were identified as those yielding an integrated signal above a threshold of 1250 counts in the Flash Analogues to Digital Converters (FADC). For comparison, a minimum ionizing particle yields about 200 FADC counts. Values slightly above 1000 FADC counts are typical for protons with a momentum of a few hundred MeV. If, within a group, more than 10 wires detected a high dE/dx hit, a decision bit was set. If this bit was set by all groups of a sector, the monopole trigger was fired. Using raw hit information of randomly triggered events, the monopole trigger was determined to have an efficiency greater than 99%.

A lead-glass electromagnetic calorimeter located outside the magnet coil covered the full azimuthal range with good hermeticity in the polar angle range of $|\cos\theta| < 0.984$. The magnet return yoke was instrumented for hadron calorimetry covering the region $|\cos\theta| < 0.99$ and was surrounded by four layers of muon chambers. Electromagnetic calorimeters close to the beam axis completed the geometrical acceptance down to 24 mrad on each side of the interaction point. These small-angle calorimeters were also used to measure the integrated luminosity by counting Bhabha events [20].

In order to trigger on the signal described in the introduction, only data collected when the monopole trigger was active were used. The data-set analysed here was recorded during the LEP2 phase with an average centre-of-mass (c.m.) energy of 206.3 GeV, and corresponded to a total integrated luminosity of 62.7 pb^{-1}.

3   Monte Carlo Simulation

The signal reaction $e^+e^- \rightarrow M\bar{M}$ was simulated at $\sqrt{s_{MC}} = 208$ GeV for monopole masses (m_M) of 45, 50, 55, 60, 65, 70, 75, 80, 85, 90, 95, 100, 101, 102, 103 and 104 GeV/c^2 with Monte Carlo (MC) event samples. Each sample contained 1000 events. Small differences in the centre-of-mass energies between the OPAL data analysed ($\sqrt{s_{min}}$= 203.6 GeV, $\sqrt{s_{max}}$= 207.0 GeV, for an average $\sqrt{s_{data}}$= 206.3 GeV) and the signal MC samples ($\sqrt{s_{MC}}$) have a negligible effect on the analysis. MM masses were scaled to the c.m. energy with the equation:

$$m_{scaled} = m_M \sqrt{\frac{s_{data}}{s_{MC}}} \tag{3}$$

This scaling is valid since dE/dx (hence detection efficiency) is a linear function of mass.

The very large value of the magnetic charge makes it impossible to use perturbative theory to calculate the MM production process. MMs were assumed to be spin 1/2 particles, produced from the e^+e^- initial state via annihilation into a virtual photon, which yields a monopole-antimonopole pair with a uniform azimuthal distribution and with the typical fermion polar angle distribution $\propto (1 + \cos^2\theta)$:

$$e^+e^- \rightarrow \gamma^* \rightarrow M\bar{M} \tag{4}$$

Since magnetic charge cannot be simulated directly, MMs were simulated as heavy electrically charged fermions with an effective charge of $(ze)_{eq} = g_D\beta$ (assuming $n = 1$). The specific ionization energy loss was computed according to Eq. 2.

A magnetic monopole interacts with a magnetic field analogously to how an electron interacts with an electric field. The Lorentz force for a magnetic monopole carrying magnetic charge g is:

$$\vec{F} = g\left(\vec{B} - \vec{v} \times \vec{E}\right) \tag{5}$$

The GEANT3 [21] based OPAL detector simulation program [22] was used to simulate the behavior of the MMs in the OPAL detector. The routines to transport the particles through the magnetic field were modified such that over a given step the change in the momentum $d\vec{p}/dt$ of the monopole was obtained by solving analytically the differential equation:

$$\frac{d\vec{p}}{dt} = g\vec{B} \tag{6}$$

The solution describes the motion of a magnetic monopole in a uniform magnetic field. The trajectory is a parabola, accelerating in the direction of the magnetic field. In the plane perpendicular to the magnetic field the motion is along a straight line, in sharp contrast to electrically charged particles, which curve in this plane.

We studied the effects of multiple scattering of the monopoles and the modelling of the electric field between the anode, cathode, and potential wires in CJ and found them to be negligible.

A software emulation of the monopole trigger was used to study its efficiency. For the simulated monopole events, the trigger efficiency was found to be essentially 100%.

The background was estimated using MC simulations of Standard Model processes, generated at $\sqrt{s}$=206 GeV. Two-fermion events $(Z^{0*}/\gamma^* \rightarrow f\overline{f}(\gamma)$ with $f = e, \mu, \tau, q)$ were simulated with KK2f [23]. For the two-photon background, the PYTHIA [24] and PHOJET [25] Monte Carlo generators were used for $e^+e^-q\overline{q}$ final states and the Vermaseren [26] and BDK [27] generators for all $e^+e^-l^+l^-$ final states. Four-fermion final states were simulated with grc4f [28], which takes into account interference between all diagrams.

All generated signal and background events were processed through the full simulation of the OPAL detector. The same event analysis chain was applied to the simulated events and to the data.

4 Data Analysis

Magnetic monopoles would distinguish themselves by their anomalously high ionization energy loss in CJ and by the different plane of curvature of the trajectory in the magnetic field, compared to electrically charged particles.

The large value of the specific energy loss $(\mathrm{d}E/\mathrm{d}x)$ of a MM in the gas of the tracking detectors would induce a saturation in most of the wire hits. With the signals from both ends of the wire saturated, it is not possible to determine the z position from charge sharing. In this case the z position is set to zero by the reconstruction program. In the MC, most MM events are seen to exhibit a mean z-coordinate near zero, because of saturation effects. Rather than trying to reconstruct the

Cut	Description	cut value
Preselection	Total charge per hit (CJ):	$\geq$ 1000 FADC
	Number of Tracks plus Clusters:	$\leq$ 18
1	The first hit wire:	$\leq$ 2
	Number of Tracks plus Clusters:	$\leq$ 4
2	Distance between the 2 sectors:	$\geq$ 8
3	Number of hits in overflow in *HighSector*:	$\geq$ 10
4	Z mean coordinate (CJ):	$\leq$ 50 cm
5	Charge per hit in the *HighSector*:	$\geq$ 3700 FADC counts
6	Charge per hit in the *SecondSector*:	$\geq$ 3000 FADC counts
	Total charge per hit (CJ):	$\geq$ 2500 FADC counts

Table 1: *List of cuts applied to the data.*

MM tracks in 3 dimensions, events were examined for the characteristic MM pattern of ionisation in the sectors of the OPAL Jet Chamber.

Pair-produced magnetic monopoles, $e^+e^- \to M\bar{M}(\gamma)$, would be expected to be produced back to back with a characteristic pattern of hits in the jet chamber. This would have resulted in an azimuthal separation of about 12 sectors between the two sectors with the highest energy deposits, called *HighSector* and *SecondSector*, with little energy deposited elsewhere in the detector.

Based on these considerations, events were rejected if the overall charge deposited on the sense wires normalised per hit was smaller than 1000 FADC counts, or if the total multiplicity of tracks plus clusters in the detector was greater than 18. The level of the FADC counts were based on gains and calibrations. We refer to these two cuts as the preselection, see Table 1.

To reject some un-modelled events, further cuts were applied: the number of reconstructed tracks plus clusters had to be no more than 4 and the first wire hit in CJ had to be one of the first two wires (cut 1 in Table 1). Table 1 summarizes the other selection criteria. We required the *HighSector* and *SecondSector* to have an azimuthal separation of at least eight sectors (cut 2) and the number of hits in overflow in the *HighSector* to be larger than or equal to 10 (cut 3). Since the typical MM signature would exhibit a mean z-coordinate near zero, the average of the z coordinate in CJ was required to be less than 50 cm (cut 4). The deposited charge per hit in *HighSector* and *SecondSector* was required to be larger than 3700 FADC and 3000 FADC counts, respectively (cut 5 and cut 6) and the total charge per hit in all the CJ sectors to be larger than 2500 FADC counts (cut 6).

The Standard Model background was dominated by Bhabha events and two-photon hadronic events, with a contribution from other two-photon events. The effect of the cuts on the samples at an average c.m. energy of $\sqrt{s}$=206.3 GeV is shown in Table 2. After applying cut 1, there was poor agreement between data and MC (see Table 2). This was because the data still contained remaining un-modelled backgrounds from beam-gas interactions, cosmic rays and detector noise. This un-modelled background was much reduced by the subsequent cuts since beam-gas interactions yield particles which mainly travel along the beam pipe and do not have the characteristic back-to-back pattern, and detector noise does not deposit large amounts of charge on the wires. The remaining difference of 15-20% between the number of events in the data and MC after cut 2 does not affect our results, as the signal is so separated from the the background that we can impose very hard cuts to remove all the background without affecting the detection efficiency.

Fig. 1 shows the distribution of two of the main variables used by the analysis after cut 2: the

cut	data	Total SM MC	Number of background events SM MC									sig. eff.(%)
			bhabha	2f	qq	$2\gamma(e)$	$2\gamma(\mu)$	$2\gamma(\tau)$	$\nu\nu$	4f	$2\gamma(q)$	
1	44491	5707	4231	0.7	0.6	75.3	2.2	71.9	1.9	57	1266	91
2	2928	2462	1927	0.1	0.3	6.0	0.1	27.5	0.3	14	487	91
3	2576	2194	1661	0.1	0.3	5.4	0.1	27.4	0.3	12.8	487	91
4	1982	1597	1405	0.0	0.0	0.4	0.0	6.9	0.0	6.4	177	91
5	2	1.2	0.5	0.0	0.0	0.0	0.0	0.1	0.0	0.0	0.6	91
6	0	0.0	0.0	0.0	0.0	0.0	0.0	0.0	0.0	0.0	0.0	91

Table 2: *The number of data and Monte Carlo events remaining after the cuts for analysed data-set collected at $\sqrt{s}$=206.3 GeV and for various MC SM background processes normalised to the integrated luminosity of the data (62.7 pb^{-1}). The last column gives the efficiencies (in percent) for the magnetic monopole MC signal simulated in the mass region between 45 GeV/c^2 and 103 GeV/c^2.*

charge per hit in the CJ sector *HighSector* and the average of the z-coordinate. The total number of data events at this stage is 2928 and the total number of the MC Standard Model events is 2462 (Table 2). Since the magnetic monopole behavior would be very different from any electrically charged SM particles, all the variables used by the analysis have a very well separated distribution for the MM signal and SM MC backgrounds. For this reason it can be seen from Table 2 that no MC background event survived the analysis cuts. Moreover the overall detection efficiency is very high ($\geq$ 90%) for almost all MM masses. In Fig. 2 the detection efficiency for pair-produced magnetic monopoles at $\sqrt{s} \cong 206$ GeV is shown as a function of m$_M$.

5 Estimates of Systematic Uncertainties

The distributions of the variables in the data and SM MC have similar shapes. The differences in the mean values are quite small. The MC modelling of the dE/dx may introduce some systematic uncertainties. These were evaluated by displacing the cut value on a given variable x from the original position x_0 to a new position $\overline{x}_0$, to reproduce on the simulated events the effect of the cut on the real data. $\overline{x}_0$ is defined by:

$$\overline{x}_0 = (x_0 - \langle x\rangle_{data})\frac{\sigma_{bkg}}{\sigma_{data}} + \langle x\rangle_{bkg} \tag{7}$$

where $\langle x\rangle_{data}$, $\langle x\rangle_{bkg}$, σ_{data} and σ_{bkg} are the mean values and the standard deviations of the distributions of the variable x for the data and the simulated background. These quantities were calculated from the x distributions of the events surviving the cuts on all the other variables used in the selection. It was verified that using the distribution of x at other stages of the selection leads to negligible changes in the values of this uncertainty.

The procedure was repeated for the main variables used in the event selection (Table 1): the number of overflows in *HighSector*, the Z mean coordinate in CJ and the charge per hit in *HighSector* and *SecondSector*. The difference between the reduced efficiency, due to the displacement of the cut, and that obtained with the nominal selection was taken as the systematic uncertainty due to the modelling of the variable under consideration. The relative systematic uncertainties in the signal

Quantity	Systematic uncertainty (%)
Number of overflows in *HighSector*	0.0 - 0.2
Z mean coordinate (CJ)	0.2 - 0.4
Charge per hit in *HighSector*	0.3 - 4.7
Charge per hit in *SecondSector*	0.2 - 2.2
Global systematic uncertainty	0.4 - 5.2
Signal MC statistics	0.6 - 0.8
Total	0.7 - 5.3

Table 3: *Summary of systematic uncertainties for the signal efficiency of the various quantities used in the analysis. The range of results corresponds to the values obtained for the different MM masses.*

efficiency associated with the various quantities are reported in Table 3. The range comes from different values obtained for the different MM masses.

At a given centre-of-mass energy the different systematic uncertainties were assumed to be independent, so that the total systematic uncertainty was calculated as the quadratic sum of the individual uncertainties. The global systematic uncertainty ranges between 0.4% and 5.2% (Table 3).

The MC statistical uncertainty, due to the limited number of signal events generated, has been computed using a binomial formula and is reported in Table 3.

6   Results and Conclusions

No magnetic monopole signal was found in this search. In Figure 3 the 95% CL upper limit on the production cross-section at an average c.m. energy of $\sqrt{s} = 206.3$ GeV is shown as a function of the monopole mass. The average upper limit on the cross-section, computed using a frequentist approach, is 0.05 pb in the mass range $45 < m_M < 102 \, \text{GeV}/\text{c}^2$. This limit is essentially independent of the mass in this range.

The computation of the cross-section is non-trivial. Nevertheless we expect the cross-section to be large. The cross-section for the pair production of Dirac Magnetic Monopoles computed assuming a naive tree-level coupling through an s-channel virtual photon, according to the effective charge $(ze)_{eq} = g_D \beta$, is around 5 orders of magnitude larger than the upper limit obtained in this experiment [14]. In this model we can thus exclude classical MMs in the mass range 45-102 GeV/c². This is a new excluded mass range for Dirac magnetic monopole searches in e⁺e⁻ interactions.

7   Acknowledgements

References

[1] P. A. M. Dirac, Proc. Roy. Soc. Lond. **A133** (1931) 60.

[2] G. Giacomelli *et al.*, hep-ex/050614.

[3] G. 't Hooft, Nucl. Phys. **B79** (1974) 276;
A. M. Polyakov, JEPT Lett. **20** (1974) 194.

[4] M. Ambrosio *et al.*, Eur. Phys. J. **C25** (2002) 511;
M. Ambrosio *et al.*, Eur. Phys. J. **C26** (2002) 163;
M. Ambrosio *et al.*, Nucl. Instr. Meth. **A486** (2002) 663.

[5] T. W. Kephart and Q. Shafi, Phys. Lett. **B520** (2001) 313.

[6] A. De Rújula, Nucl. Phys. **B435** (1995) 257;
S. Cecchini *et al.*, Radiat. Meas. **40** (2005) 405, hep-ex/0503003.

[7] L.W. Alvarez *et al.*, Science **167** (1970) 701.

[8] G. R. Kalbfleisch *et al.*, Phys. Rev. Lett. **85** (2000) 5292;
B. Abbott *et al.*, Phys. Rev. Lett. **81** (1998) 5954;
K. A. Milton, Rept. Prog. Phys. **69** (2006) 1637.

[9] A. Aktas *et al.*, H1 Collab., Eur. Phys. J. **C41** (2005) 133.

[10] S. P. Ahlen, Phys. Rev. **D17** (1978) 229.

[11] G. Giacomelli, Riv. Nuovo Cim. **7, no.12** (1984) 1.

[12] G. Giacomelli and P. Giacomelli, Riv. Nuovo Cim. **16, no.3** (1993) 1-58.

[13] M. Bertani *et al.*, Europhys. Lett. **12** (1990) 613;
A. Abulencia *et al.*, Phys. Rev. Lett. **96** (2006) 201801.

[14] K. Kinoshita *et al.*, Phys. Rev. **D46** (1992) R881;
J. L. Pinfold *et al.*, Phys. Lett. **B316** (1993) 407.

[15] B. Abbott *et al.*, Phys. Rev. Lett. **81** (1998) 524.

[16] M. Acciarri *et al.*, Phys. Lett. **B345** (1995) 609.

[17] G. Abbiendi *et al.*, OPAL Collab., Phys. Lett. **B572** (2003) 8;
R. Akers *et al.*, OPAL Collab., Z. Phys. **C67** (1995) 203;
K. Ackerstaff *et al.*, OPAL Collab., Phys. Lett. **B433** (1998) 195.

[18] K. Ahmet *et al.*, OPAL Collab., Nucl. Instr. Meth. **A305** (1991) 275;
K. Ahmet *et al.*, OPAL Collab., Nucl. Instr. Meth. **A283** (1989) 492.

[19] O. Biebel *et al.*, Nucl. Instr. Meth. Phys. Res. **A323** (1992) 169.

[20] G. Abbiendi *et al.*, OPAL Collab., Eur. Phys. J. **C14** (2000) 373;
G. Abbiendi *et al.*, OPAL Collab., Eur. Phys. J. **C45** (2006) 1.

[21] R. Brun *et al.*, GEANT3 user's guide, CERN DD/EE/84-1, 1984.

[22] J. Allison *et al.*, Nucl. Inst. Meth. **A317** (1992) 47.

[23] S. Jadach *et al.*, Comput. Phys. Commun. **130** (2000) 260.

[24] T. Sjostrand and M. Bengtsson, Comp. Phys. Comm. **43** (1987) 367;
T. Sjostrand, Comp. Phys. Comm. **135** (2001) 238.

[25] R. Engel and J. Ranft, Phys. Rev. **D54** (1996) 4244;
R. Engel, Z. Phys. **C66** (1995) 203.

[26] R. Bhattacharya, J. Smith and G. Grammer, Phys. Rev. **D15** (1977) 3267;
J. Smith *et al.*, Phys. Rev. **D15** (1977) 3280; Phys. Rev. **D19** (1979) 137.

[27] F. A. Berends, P. H. Daverveldt and R. Kleiss, Nucl. Phys. **B253** (1985) 421; Comp. Phys. Comm. **40** (1986) 271, 285, 309.

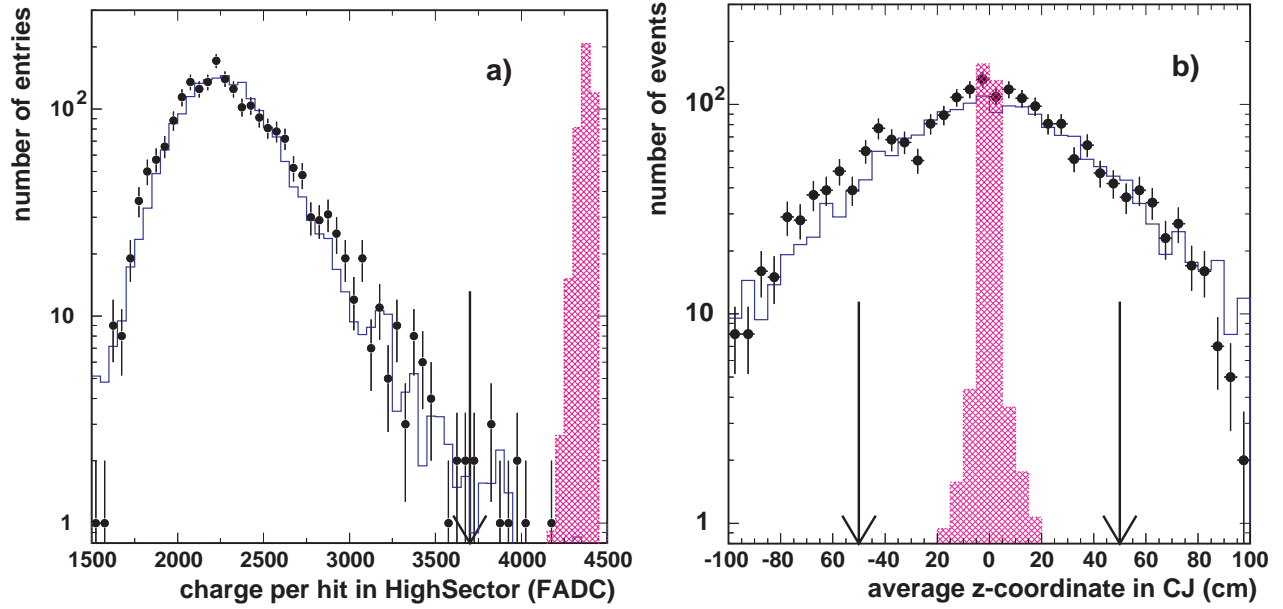[28] J. Fujimoto *et al.*, Comp. Phys. Comm. **100** (1997) 128.

Figure 1: Global event properties after applying cut 2. The solid histogram is the generated Standard Model MC background, the filled histogram is the MC magnetic monopole signal and the points are the data. a) charge deposited in the *HighSector* in CJ (FADC); b) average z-coordinate of all hits in the jet chamber. Most MM events are seen to exhibit a mean z-coordinate near zero, because of the saturation effects mentioned in Sect. 4. The arrows in each plot show the cuts applied in the analysis.
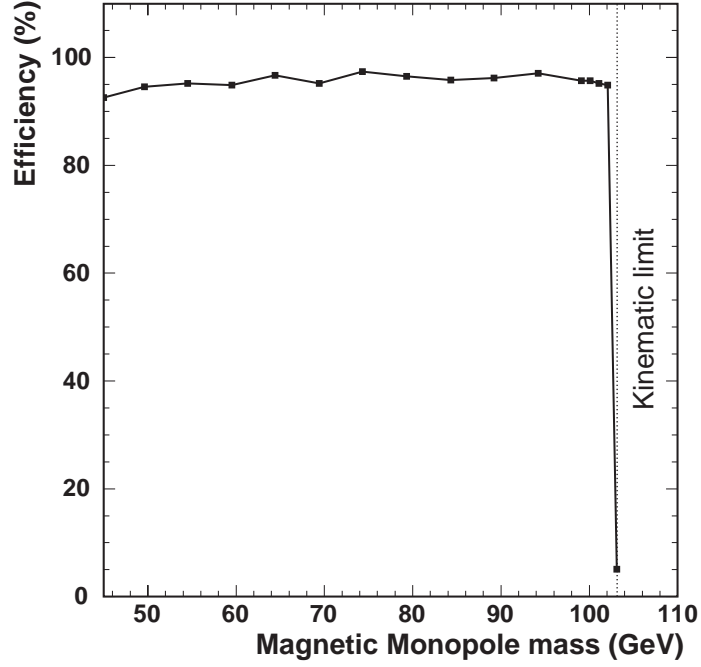
Figure 2: Monte Carlo estimate of the selection efficiency as a function of the monopole mass at $\sqrt{s}$=206.3 GeV. The dotted line is the kinematic limit.
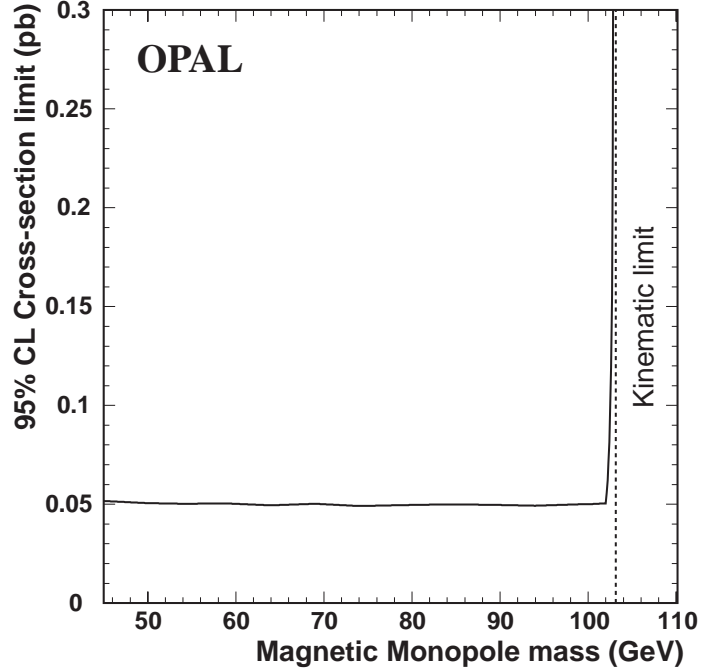

Figure 3: The model-independent 95% C.L. upper limit on the pair-production cross-section of magnetic monopoles in e^+e^- collisions at LEP2 at $\sqrt{s}$=206.3 GeV (plotted vs MM mass).